

Fiber-Based Electret Nanogenerator with a Semisupported Structure for Wearable Electronics

Li'ang Zhang, Qianqian Chen, Xiaoyu Huang, Xiaofeng Jia, Bolang Cheng, Longfei Wang,* and Yong Qin*



Cite This: <https://doi.org/10.1021/acsami.1c16255>



Read Online

ACCESS |



Metrics & More



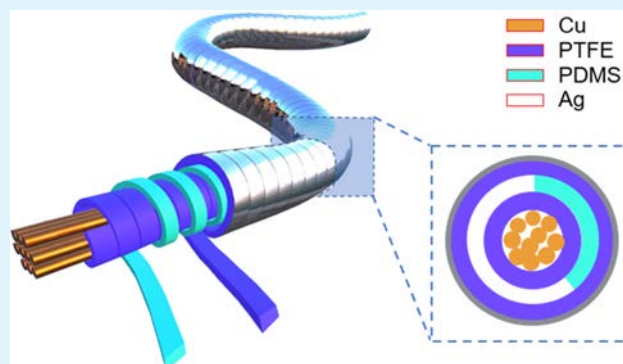
Article Recommendations



Supporting Information

ABSTRACT: Fiber-based nanogenerators have great potential applications in wearable electronics such as portable nanodevices, e-skin, and artificial intelligence system. Here, we report a kind of fiber-based electret nanogenerator (FENG) with a semisupported core-shell structure. Owing to its unique structure, the open-circuit voltage and short-circuit current of the FENG reach 40 V and 0.6 μA , respectively, under a short working distance ($\sim 25 \mu\text{m}$). No obvious degradation of the output performance under a long-time continuous work ($>16 \text{ h}$) and different humidity environments (20–95%) is observed, which demonstrates the FENG's good reliability and stability. Many universal materials, such as cotton rope, conductive sewing thread, and polyvinyl chloride tube, have been successfully used to fabricate FENG. Meanwhile, the FENG-based wearable fabric has been successfully developed to effectively harvest mechanical energy of human motion. The FENG is highly effective, reliable, and stable, promoting the development of fiber-based nanogenerators and their applications in self-powered wearable electronics.

KEYWORDS: nanogenerator, fiber-based nanogenerator, electret, energy harvesting, self-powered wearable electronics



INTRODUCTION

Fiber-based nanogenerators have been receiving extensive attention due to their potential for wearable electronic devices with *in situ* energy harvesting from human motions.^{1–8} Previous reports of fiber-based nanogenerators mainly focus on two kinds of nanogenerators with different mechanisms. One is the piezoelectric nanogenerator, which can convert weak mechanical energy into electrical energy by means of piezoelectric materials such as ZnO,^{9–12} poly(vinylidene difluoride),^{13–16} or piezoceramics.^{17,18} The electrical output of these piezoelectric nanogenerators under weak mechanical stimuli is not high enough for powering some wearable electronics and lacks flexibility, which limits their further applications. The other is the triboelectric nanogenerator based on the coupling effect of contact electrification and electrostatic induction.^{19–27} The advantage of the fiber-based triboelectric nanogenerator is the high electrical output,^{19,25} lightweight, and excellent flexibility.^{27,28} In general, the working of the triboelectric nanogenerator requires the effective contact of two triboelectric materials, the displacement of which is usually called working distance.²⁹ However, the working distances of most triboelectric nanogenerators are usually on the orders of millimeters to centimeters, which limit their applications in the field of ultrathin nanogenerators and sensing. A few reports of triboelectric nanogenerators with

short working distances ($\sim 5^{30}$ and $\sim 10 \mu\text{m}^{22}$) have been reported, which are beneficial to the energy harvesting and sensing of weak movement. Nevertheless, making the high-robust nanogenerator having an effective and stable output under a short working distance still needs further study.

An electret film is widely adopted in nanogenerators, sensors, and microelectromechanical systems due to its high charge storage capability and quasi-permanent stability.^{31,32} Introducing air bubbles or a similar structure into electret materials is an effective way to improve the performance of the nanogenerator under a reduced working distance.^{29,33–41} When the electret materials are polarized, opposite electric charges will accumulate at inner top and bottom surfaces of the air bubbles and form giant quasi-dipoles. These charges can be stored for a long time and are difficult to be dissipated in a humid environment, resulting in a high output, high stability, and reliability of the nanogenerator.^{33,37} In addition, during the working process of the above devices, there is unnecessary

Received: August 25, 2021

Accepted: September 10, 2021

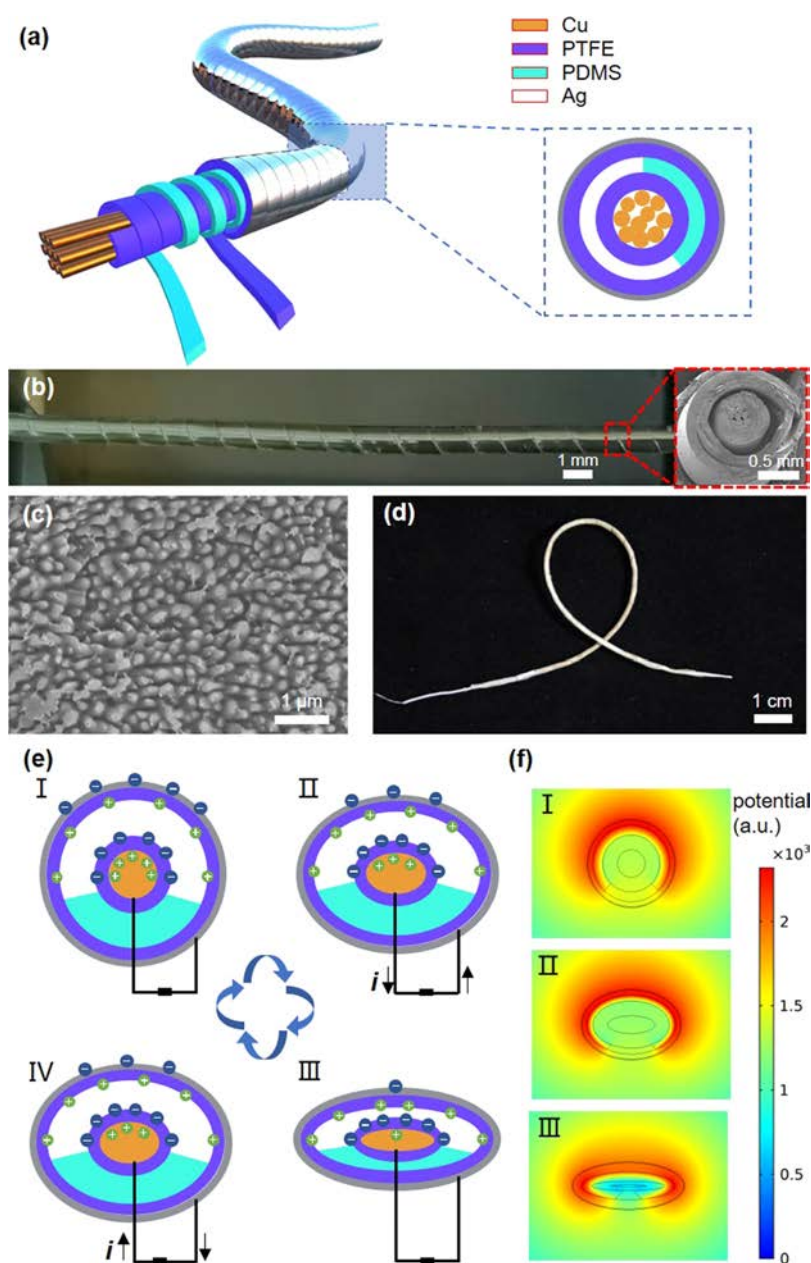


Figure 1. Prototype and working mechanism of the FENG. (a) Schematic illustration of the structure of the FENG. (b) Photograph of the FENG. The inset shows the cross section of the FENG. (c) Morphology of the treated surface of the PTFE film. (d) Image of the bending FENG shows its flexibility. (e) Schematic diagrams show the working principle of FENG. (f) Simulation of the potential distribution of FENG under open-circuit conditions using COMSOL software.

contact between inner top and bottom surfaces of the air bubbles. Thus, effective electromechanical energy conversion can be realized under a reduced working distance. If the air bubble technology of the electret can be utilized to fabricate fiber-based nanogenerators, it will contribute greatly to the development of self-powered wearable electronics and their wearable power sources.

Herein, a kind of fiber-based electret nanogenerator (FENG) with a semisupported core–shell structure has been developed, which exhibits high reliability, stability, and universality. The FENG can output 40 V open-circuit voltage and $0.6 \mu\text{A}$ short-circuit current under a short working distance ($\sim 25 \mu\text{m}$). Moreover, it can work continuously and effectively at various humidity ambiances (20–95%) for a long time without obvious degradation. Meanwhile, many kinds of

universal materials such as cotton rope, polyvinyl chloride (PVC) tube, and conductive sewing thread have been successfully fabricated into FENG. Furthermore, wearable FENGs have been successfully developed, which demonstrated their effectiveness in harvesting the mechanical energy of human moment.

RESULTS AND DISCUSSION

Fabrication of the FENG. Figure 1a shows the schematic illustration of the FENG, which consists of an inner electrode (Cu), inner electret layer poly(tetrafluoroethylene) (PTFE), supporting spacer poly(dimethylsiloxane) (PDMS), outer electret layer (PTFE), and outer electrode (Ag). First, commercial PTFE-insulated Cu wires are prepared. The PTFE insulation ($150 \mu\text{m}$) is chosen as an inner electret

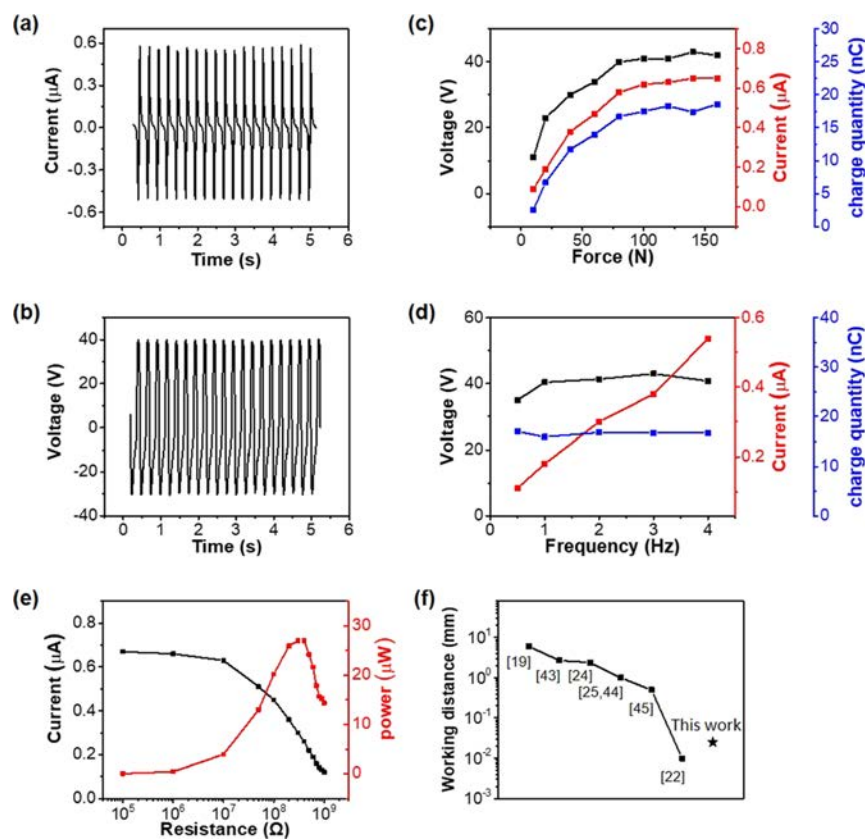


Figure 2. Output performance of the FENG. The I_{sc} (a) and V_{oc} (b) of the FENG under periodical stimulation with a force of 80 N and a frequency of 4 Hz. (c) Peak V_{oc} , I_{sc} , and Q_{sc} of the FENG under various forces (frequency: 4 Hz). (d) Peak V_{oc} , I_{sc} , and Q_{sc} of the FENG at various frequencies (force: 80 N). (e) Variation of the peak current and output peak power vs the external loading resistances. (f) Working distance of the FENG and some representative fiber-based core–shell triboelectric nanogenerators.

layer due to its high charge storage stability. The surface of PTFE insulation is treated by a reactive ion etching (RIE) machine to increase its surface roughness. Second, a PDMS strap with a thickness of 100 μm and a width of 1 mm is twinned on the PTFE-insulated Cu wires, which introduces an air gap between the inner and outer electret layers and ensures the core and shell coaxially. Meanwhile, owing to the PDMS supporting layer, the pressed air gap could recover quickly when the compressive stress removes. Third, a PTFE strap with a thickness of 50 μm and a width of 3 mm is prepared. One surface of the PTFE strap is treated by an RIE machine to increase its roughness, as shown in Figure 1c. The surface roughness modification could remain for a long time (Figure S1). The other surface of the PTFE strap is metalized by magnetron sputtering as the outer electrode. Then, the treated PTFE strap tightly entwinds on the fiber with the metalized surface outside. Finally, PDMS as the package is coated on the FENG by the dip-coating method to improve the FENG's reliability. The detailed fabrication process is shown in the Experimental Section. Images of the as-prepared FENG are shown in Figure 1b,d, and the inset shows the cross-sectional view of the FENG, which illustrates the high axiality and flexibility of the FENG.

Charging of the FENG. The FENG needs charging by the contact charging method (Figure S2). By applying a high voltage of 10 kV between inner and outer electrodes of the FENG at a temperature of 100 $^{\circ}\text{C}$ for 10 min, the air breakdown in the FENG occurs. Then, positive and negative charges will accumulate on the inner and outer electret layers,

respectively. The part of electret layers contacting with the PDMS supporting spacer cannot be charged because of lacking air gap. The thermally stimulated discharge current of charged/uncharged samples is measured, which exhibits the effectiveness of the contact charging method (Figure S3). Meanwhile, the roughness of the PTFE surface versus its charge storage performance has been studied, as shown in Figure S4. The result shows that the charge decay of the treated PTFE film is obviously slower than that of the untreated film, which demonstrates the well charge storage property of the rough PTFE films.

Working Mechanism of the FENG. The working mechanism of the FENG in the radial direction slice is shown in Figure 1e. The negative/positive charges presented at the inner/outer electret layer could be regarded as giant quasi-dipoles. In the original state, there are opposite charges presented at the inner/outer electrodes induced by the giant quasi-dipoles, as shown in Figure 1e-I. When the FENG is pressed by an external force, most of the deformation is concentrated on the PDMS since the PDMS supporting spacer is the main elastomer of the FENG. Thus, the thickness of the air gap is effectively reduced during the compressing process, which decreases the polarization intensity of the giant quasi-dipoles. Hence, a potential will be generated between the two electrodes, which leads to electrons flowing from the outer electrode to the inner electrode, as shown in Figure 1e-II. In the compressed state, the thickness of the air gap reaches minimum, and a new electrostatic equilibrium is established, as shown in Figure 1e-III. During the releasing process, the

thickness of the air gap will increase due to the elasticity of the PDMS supporting spacer, resulting in an inverse potential and hence a reverse flow of electrons, as shown in Figure 1e-IV. When the pressure is removed, the FENG returns to its initial state and a working cycle is completed. As a result, an instantaneous alternating current through the external load will be generated via periodically compressing and releasing of the FENG. Figure 1f shows the simulated electrostatic potential distributions of various working states of FENG, which further illustrate the working mechanism of FENG. Actually, the FENG in the axial direction slice can be regarded as several nanogenerators in parallel (Figure S5). During the working process, the deformed parts can output an alternating electrical signal via periodically compressing and releasing, and the undeformed parts have no contribution on the charge-transfer process.

Output Performance of the FENG. The schematic diagram of the test equipment is shown in Figure S6. A poly(methyl methacrylate) plate ($5 \times 5 \text{ cm}^2$) fixed at the end of a spring is periodically driven by a linear motor. In this way, a constant force can be applied on the fiber in the radial direction to press and release the FENG. With a compressive force of 80 N and a frequency of 4 Hz, the short-circuit current (I_{sc}) and open-circuit voltage (V_{oc}) of the FENG ($\sim 5 \text{ cm}$ in length) reach $0.6 \mu\text{A}$ (Figure 2a) and 40 V (Figure 2b), respectively. Meanwhile, the force-dependent electrical outputs of the FENG, including V_{oc} , I_{sc} , and short-circuit charge transfer (Q_{sc}), are characterized at a frequency of 4 Hz (Figure 2c). As a result, when the force is lower than 80 N, it is a nearly linear relation between the output of FENG and the compressive force. When the force is larger than 80 N, the outputs increase slowly with the increasing force and gradually reach saturation. The relationship between the output performance of FENG and the frequency of stimulation is shown in Figure 2d. Under a compressive force of 80 N, we find that the I_{sc} gradually increases (from 0.11 to $0.55 \mu\text{A}$), whereas the V_{oc} and Q_{sc} are relatively stable as the frequency increased from 0.5 to 4 Hz. Under high-frequency mechanical agitation, the positive and negative potentials on electret layers (PTFE) are not completely neutralized, which leads to an accumulation of residual charges on the electrodes and results in an increased current.⁴² Nevertheless, the frequency of stimulation would not change the deformation quantity of the air gap of FENG, which is related to the stable output V_{oc} and Q_{sc} of FENG. In addition, the relationship between the output voltage of FENG and the thickness of the inner PTFE layer is shown in Figure S7. The FENG with thicker PTFE could reach a higher output.

In order to find out the equivalent internal resistance of the FENG and the corresponding maximum output power, the load peak currents are measured under a series of external loads at a frequency of 4 Hz and a force of 103.3 N. According to the power formula: $P = I^2R$, the maximum output peak power of the FENG reaches $\sim 27 \mu\text{W}$ with an external load of $400 \text{ M}\Omega$ (Figure 2e). Owing to the semisupporting structure of the FENG, full contact between the core layer and the shell layer of FENG is not necessary. The FENG can provide effective and stable outputs under a working distance of $\sim 25 \mu\text{m}$ (Figure S8), which is much shorter than the thickness of the air gap ($100 \mu\text{m}$) and beneficial to the energy harvesting of slight vibration or weak movement. Figure 2f shows the working distance of some representative fiber-based core-shell structure triboelectric nanogenerators.^{19,22,24,25,43-45} The

working distance of most core-shell triboelectric nanogenerators is on the order of millimeters. Compared with them, the FENG has the much smaller working distance, which is beneficial to the harvesting or detection of weak mechanical movements with small amplitude.

Stability and Reliability of FENGs. The stability and reliability at various humidity environments of FENGs are examined. After continuous working for 1000 min (about 2.4×10^5 cycles), there is no obvious degradation of V_{oc} (Figure 3a). Besides, as shown in Figure S9, there is only a little

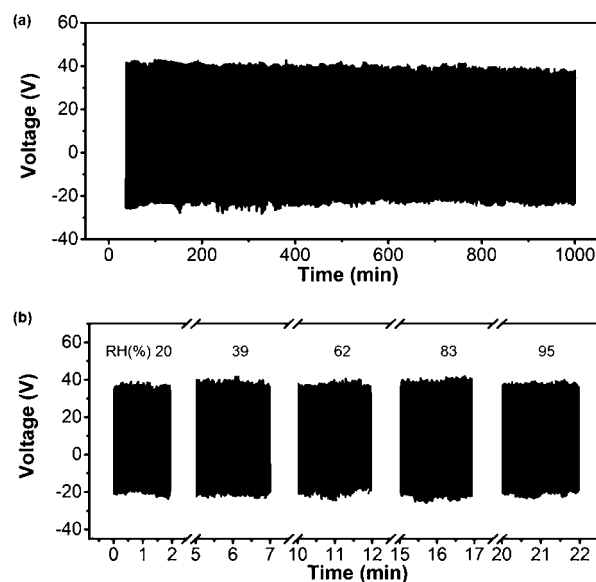


Figure 3. Stability and reliability of the FENG. (a) Continuous testing of the FENG for 1000 min shows its stability and durability. (b) FENG works at different humidity ambiances, exhibiting its reliability.

degradation of the V_{oc} of the FENG after 2 months. These results demonstrate the stability of the FENG, which is mainly attributed to the well charge storage capacity of the electret (PTFE) and the semisupporting structure of the FENG (easily returns to its original state after being deformed by an external force). Moreover, owing to the well encapsulation, the FENG can work effectively in various humidity environments (relative humidity, 20–95%) and nearly without performance degradation (Figure 3b), which shows the high reliability of the FENG. The detailed processes of the measurements in various humidity ambiances are shown in Figure S10. In addition, after being washed in water and naturally dried for three times, the FENG still has a stable output, which further demonstrates the reliability of the FENG (Figure S11).

FENGs Based on Other Fibers or Tubes. To show that the FENG is not limited to metal fibers, we fabricate the FENGs based on other fibers or tubes such as cotton rope, conductive sewing thread, and PVC tube (Figure 4). These FENGs can effectively harvest mechanical energy and give stable outputs. As shown in Figure 4a, the output I_{sc} ($0.34 \mu\text{A}$) and V_{oc} (15.8 V) of the FENG based on cotton rope can be obtained with a periodic stimulation at a frequency of 4 Hz and a force of $\sim 80 \text{ N}$. Meanwhile, with the same periodic stimulation, the output I_{sc} (0.15, $0.26 \mu\text{A}$) and V_{oc} (8.6, 35.1 V) of FENGs based on conductive sewing thread and PVC tube are achieved, respectively (Figure 4b,c). In addition, the PDMS semisupporting layer of the FENG can support the core and shell materials and provide elasticity at the same time.

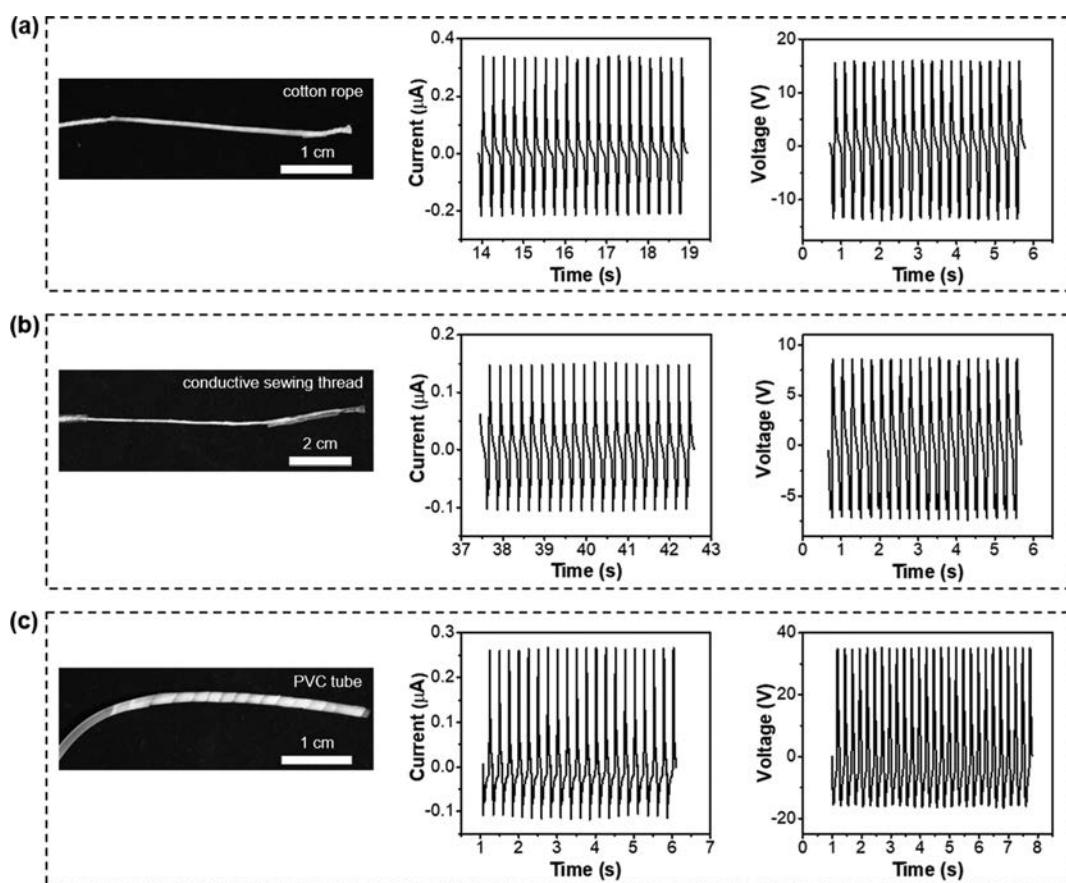


Figure 4. FENGs based on other fibers or tubes. (a–c) Photos and electrical outputs (at a frequency of 4 Hz and a force of ~ 80 N) of the FENGs based on (a) cotton rope, (b) conductive sewing thread, and (c) PVC tube.

Thus, the choice of shell materials of the FENG is more extensive. For example, PTFE, fluorinated ethylene propylene, cycloolefin copolymers, and other polymers with various elasticities are applicable, which is beneficial for the applications of fiber-based nanogenerators in textile-based wearable electronics.

Application of the FENG in Wearable Electronics.

Energy harvesting from human motion is an efficient solution for the power supply of wearable electronics. In order to demonstrate the potential of FENGs for wearable electronics, we have woven the FENGs into the fabrics and worn them on the human body (Figure 5a,b). As a result, the fabrics can effectively harvest mechanical energy from human motion. When the wearer is running, a rectified I_{sc} ($\sim 4 \mu\text{A}$) and a V_{oc} (~ 47 V) can be generated. Meanwhile, the electric energy harvested by the fabric through slight hand flapping can light up 10 light-emitting diodes (LEDs) (Figure 5c and Video S1). More importantly, the self-powered wearable electronics is achieved by integrating the electronic watch, energy-harvesting fabric (lower right inset of Figure 5d), and the energy management circuit (upper left inset of Figure 5d) on the wrist. The energy generated by the fabric could be stored in a capacitor ($10 \mu\text{F}$) through rectification, which can power the electronic watch when the voltage of the capacitor is higher than 3 V. The working process of the self-powered wearable electronic is shown in Video S2. Figure 5d shows the variation of the voltage of the capacitor during the charging and discharging process. These results show the potential of the FENGs for self-powered wearable electronics.

CONCLUSIONS

In summary, we have developed a kind of FENG with a semisupported core–shell structure. The I_{sc} and V_{oc} reach $0.6 \mu\text{A}$ and 40 V, respectively, under a short working distance ($\sim 25 \mu\text{m}$). The outputs of the FENG basically remain stable under a long-time continuous work (>16 h) and different humidity environments (relative humidity, 20–95%), which indicates the high reliability and stability of the FENG. Furthermore, the FENG can be fabricated on various fibers or tubes (such as cotton rope, conductive sewing thread, and PVC tube), which is beneficial for the integration of nanogenerators on textiles. More importantly, the wearable energy-harvesting fabric has been developed, which can effectively scavenge mechanical energy of human motion and power the portable electronics. All these advantages of the FENG show their great potential for self-powered wearable electronics.

EXPERIMENTAL SECTION

Preparation of the Treated PTFE Strap. The commercial PTFE film (thickness of $50 \mu\text{m}$) is first ultrasonically cleaned with acetone, ethanol, and deionized water for 15 min, respectively, and then, the film is dried at 80°C in an oven. Subsequently, one surface of the film is etched by an RIE machine for 1 min (10 sccm of O_2 , 30 sccm of CF_4 , and 15 sccm of Ar, 6 Pa, and 200 W input power). Then, a layer of Ag is deposited on the other surface of the PTFE film by magnetron sputtering for 5 min (50 sccm of Ar, 0.5 Pa, and 100 W input power). Finally, the film is cut into strap shape with a width of 3 mm.

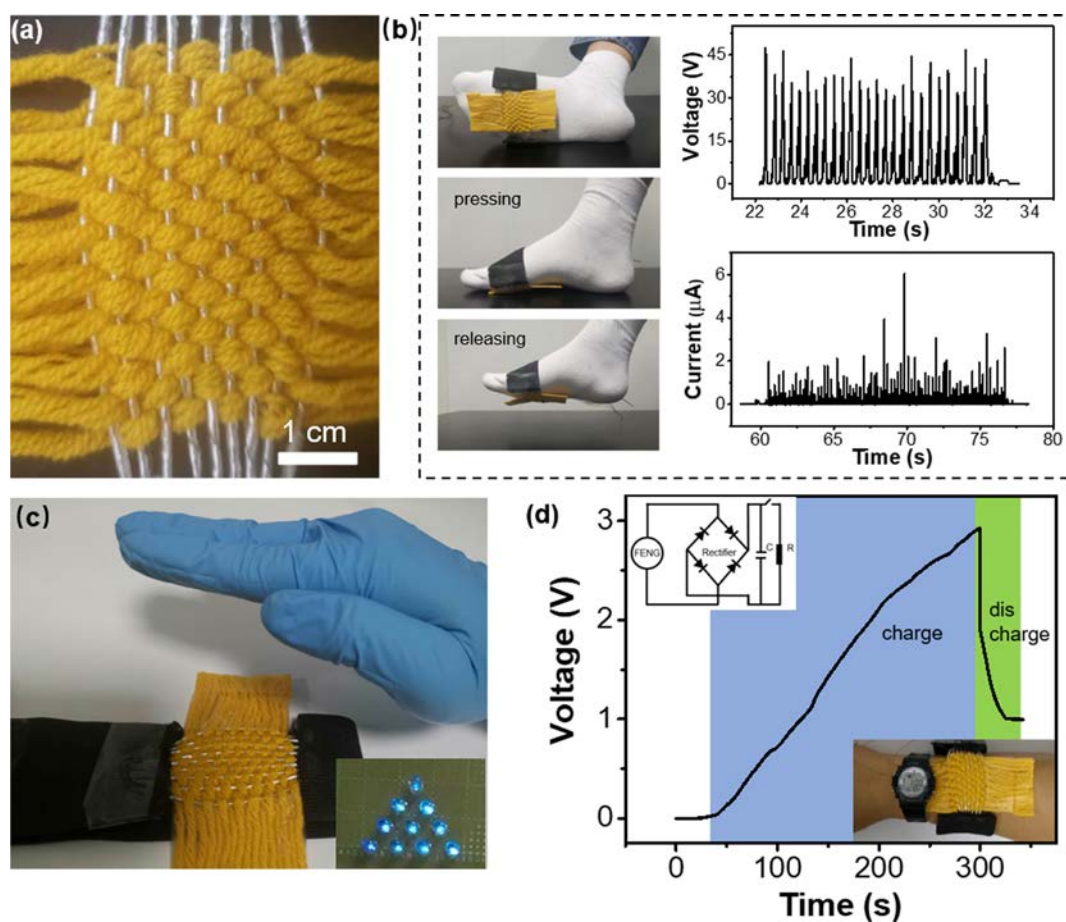


Figure 5. Application of the FENG in wearable electronics. (a) Image of the energy-harvesting fabric woven based on the FENGs. (b) Photograph of the energy-harvesting fabric wrapped on the foot and the corresponding output performance. (c) The LEDs are lighted up by slight hand flapping the energy-harvesting fabric. (d) Charging curves of a capacitor by hand flapping the energy-harvesting fabric and the subsequent discharging process of powering an electronic watch ($50 \mu\text{W}$). The upper left inset shows the energy management circuit diagram. The lower right inset shows the image of a self-charging system that harvests human motion energy to power an electronic watch.

Enwinding Process of PDMS and PTFE. The enwinding process is finished by a home-made device. During the enwinding process, both sides of the core fiber are fixed in clamps to keep the fiber vertical. One end of the strap (PDMS or PTFE) is fixed on the fiber by double-side adhesive tape. Also, a holder is used to keep the PDMS strap straight at an angle of 40° to the vertical fiber. Then, by pulling up and rotating the fiber at uniform speeds, the PDMS and PTFE straps would uniformly enwind the fiber to form spiral and tube shapes, respectively.

Fabrication of the FENGs. First, the commercial PTFE-insulated Cu wire is prepared and cleaned. Subsequently, the surface is etched by an RIE machine for 1 min (10 sccm of O_2 , 30 sccm of CF_4 , and 15 sccm of Ar, 6 Pa, and 200 W input power). For the FENGs based on cotton rope, conductive sewing thread, and PVC tube, the treated PTFE strap has tightly enwound the fiber basement (cotton rope, conductive sewing thread, and PVC tube) to form a tube shape with the metallized surface inside. Second, the uncured PDMS is coated on glass by the blade-coating method. After curing under 80°C for 3 h, the PDMS film with a uniform thickness of $100 \mu\text{m}$ is achieved. Then, the PDMS film is cut into straps with a width of 1 mm. Subsequently, the PDMS strap enwinds the fiber to form a spiral structure by a home-made device. Third, the treated PTFE strap enwinds coaxially by the same enwinding method to form a tube shape with the metallized surface outside. Fourth, the device is packaged in PDMS by the dip-coating method.

Characterization and Measurement. A Hitachi S-4800 field-emission scanning electron microscope is used to characterize the surface morphology of the etched PTFE film and the cross section of

the FENG. A probe electrostatic voltmeter (Monroe Electronics, model 279) is used to detect the surface electrostatic voltage of the PTFE film. COMSOL software is adopted to simulate the electrostatic potential distribution of FENG. A linear motor (LinMot E1100) is applied to provide the periodic pressure on the FENG. A force meter (Bengbu Sensor System Engineering Co. LTD., JHBM-H1) is adopted to measure the force applied to the FENG. A low-noise current amplifier (Stanford Research System, SR570) is used to measure the short-circuit current of FENG, and the open-circuit voltage of FENG is measured by a data acquisition card (National Instrument BNC-2120).

■ ASSOCIATED CONTENT

Supporting Information

The Supporting Information is available free of charge at <https://pubs.acs.org/doi/10.1021/acsami.1c16255>.

Continuity of the RIE treatment effect; schematic diagrams for the charging process, working process, and experimental setup; thermally stimulated depolarization current curve and surface potential of the FENG; effect of thickness of inner PTFE; deformation of the FENG under a force of 100 N; and experimental details about stability and reliability of the FENG (PDF)

Process of LEDs lighted up by the FENG fabric (MP4)

Demonstration of the electronic watch powered by the FENG fabric (MP4)

AUTHOR INFORMATION

Corresponding Authors

Longfei Wang – Beijing Institute of Nanoenergy and Nanosystems, Chinese Academy of Sciences, Beijing 101400, China; Email: lfwang12@binn.cas.cn

Yong Qin – Institute of Nanoscience and Nanotechnology, School of Materials and Energy, Lanzhou University, Lanzhou 730000, China; orcid.org/0000-0002-6713-480X; Email: qinyong@lzu.edu.cn

Authors

Li'ang Zhang – Institute of Nanoscience and Nanotechnology, School of Materials and Energy, Lanzhou University, Lanzhou 730000, China

Qianqian Chen – Institute of Nanoscience and Nanotechnology, School of Materials and Energy, Lanzhou University, Lanzhou 730000, China

Xiaoyu Huang – Institute of Nanoscience and Nanotechnology, School of Materials and Energy, Lanzhou University, Lanzhou 730000, China

Xiaofeng Jia – Institute of Nanoscience and Nanotechnology, School of Materials and Energy, Lanzhou University, Lanzhou 730000, China

Bolang Cheng – Institute of Nanoscience and Nanotechnology, School of Materials and Energy, Lanzhou University, Lanzhou 730000, China

Complete contact information is available at:
<https://pubs.acs.org/10.1021/acsami.1c16255>

Notes

The authors declare no competing financial interest.

ACKNOWLEDGMENTS

This work was supported by the Joint Fund of Equipment Preresearch and Ministry of Education (no. 6141A02022518), the National Program for Support of Top-notch Young Professionals, and the Fundamental Research Funds for the Central Universities (no. lzujbky-2020-sp08).

REFERENCES

- (1) Huang, L.; Lin, S.; Xu, Z.; Zhou, H.; Duan, J.; Hu, B.; Zhou, J. Fiber-Based Energy Conversion Devices for Human-Body Energy Harvesting. *Adv. Mater.* **2019**, *32*, 1902034.
- (2) Zeng, W.; Shu, L.; Li, Q.; Chen, S.; Wang, F.; Tao, X.-M. Fiber-Based Wearable Electronics: A Review of Materials, Fabrication, Devices, and Applications. *Adv. Mater.* **2014**, *26*, 5310–5336.
- (3) Zaarour, B.; Zhu, L.; Huang, C.; Jin, X.; Alghafari, H.; Fang, J.; Lin, T. A Review on Piezoelectric Fibers and Nanowires for Energy Harvesting. *J. Ind. Text.* **2021**, *51*, 297.
- (4) Dong, K.; Peng, X.; Wang, Z. L. Fiber/Fabric-Based Piezoelectric and Triboelectric Nanogenerators for Flexible/Stretchable and Wearable Electronics and Artificial Intelligence. *Adv. Mater.* **2019**, *32*, 1902549.
- (5) Fan, W.; He, Q.; Meng, K.; Tan, X.; Zhou, Z.; Zhang, G.; Yang, J.; Wang, Z. L. Machine-Knitted Washable Sensor Array Textile for Precise Epidermal Physiological Signal Monitoring. *Sci. Adv.* **2020**, *6*, No. eaay2840.
- (6) Cui, N.; Liu, J.; Gu, L.; Bai, S.; Chen, X.; Qin, Y. Wearable Triboelectric Generator for Powering the Portable Electronic Devices. *ACS Appl. Mater. Interfaces* **2015**, *7*, 18225–18230.
- (7) Mukhopadhyay, S. C. Wearable Sensors for Human Activity Monitoring: A Review. *IEEE Sens. J.* **2015**, *15*, 1321–1330.
- (8) Zi, Y.; Wang, Z. L. Nanogenerators: An Emerging Technology Towards Nanoenergy. *APL Mater.* **2017**, *5*, 074103.
- (9) Qin, Y.; Wang, X.; Wang, Z. L. Microfibre-Nanowire Hybrid Structure for Energy Scavenging. *Nature* **2008**, *451*, 809–813.
- (10) Lee, M.; Chen, C.-Y.; Wang, S.; Cha, S. N.; Park, Y. J.; Kim, J. M.; Chou, L.-J.; Wang, Z. L. A Hybrid Piezoelectric Structure for Wearable Nanogenerators. *Adv. Mater.* **2012**, *24*, 1759–1764.
- (11) Zhang, L.; Bai, S.; Su, C.; Zheng, Y.; Qin, Y.; Xu, C.; Wang, Z. L. A High-Reliability Kevlar Fiber-ZnO Nanowires Hybrid Nanogenerator and its Application on Self-Powered UV Detection. *Adv. Funct. Mater.* **2015**, *25*, 5794–5798.
- (12) Li, Z.; Wang, Z. L. Air/Liquid-Pressure and Heartbeat-driven Flexible Fiber Nanogenerators as a Micro/Nano-power Source or Diagnostic Sensor. *Adv. Mater.* **2011**, *23*, 84–89.
- (13) Song, S.; Yun, K.-S. Design and Characterization of Scalable Woven Piezoelectric Energy Harvester for Wearable Applications. *Smart Mater. Struct.* **2015**, *24*, 045008.
- (14) Lu, X.; Qu, H.; Skorobogatiy, M. Piezoelectric Micro- and Nanostructured Fibers Fabricated from Thermoplastic Nanocomposites Using a Fiber Drawing Technique: Comparative Study and Potential Applications. *ACS Nano* **2017**, *11*, 2103–2114.
- (15) Ahn, Y.; Song, S.; Yun, K.-S. Woven Flexible Textile Structure for Wearable Power-Generating Tactile Sensor Array. *Smart Mater. Struct.* **2015**, *24*, 075002.
- (16) Gao, H.; Minh, P. T.; Wang, H.; Minko, S.; Locklin, J.; Nguyen, T.; Sharma, S. High-Performance Flexible Yarn for Wearable Piezoelectric Nanogenerators. *Smart Mater. Struct.* **2018**, *27*, 095018.
- (17) Lee, Y. B.; Han, J. K.; Noothongkaew, S.; Kim, S. K.; Song, W.; Myung, S.; Lee, S. S.; Lim, J.; Bu, S. D.; An, K.-S. Toward Arbitrary-Direction Energy Harvesting through Flexible Piezoelectric Nanogenerators Using Perovskite PbTiO₃ Nanotube Arrays. *Adv. Mater.* **2017**, *29*, 1604500.
- (18) Zhang, M.; Gao, T.; Wang, J.; Liao, J.; Qiu, Y.; Xue, H.; Shi, Z.; Xiong, Z.; Chen, L. Single BaTiO₃ Nanowires-Polymer Fiber Based Nanogenerator. *Nano Energy* **2015**, *11*, 510–517.
- (19) Wang, J.; Li, S.; Yi, F.; Zi, Y.; Lin, J.; Wang, X.; Xu, Y.; Wang, Z. L. Sustainably Powering Wearable Electronics Solely by Biomechanical Energy. *Nat. Commun.* **2016**, *7*, 12744.
- (20) Gong, W.; Hou, C.; Zhou, J.; Guo, Y.; Zhang, W.; Li, Y.; Zhang, Q.; Wang, H. Continuous and Scalable Manufacture of Amphibious Energy Yarns and Textiles. *Nat. Commun.* **2019**, *10*, 868.
- (21) Dong, K.; Peng, X.; An, J.; Wang, A. C.; Luo, J.; Sun, B.; Wang, J.; Wang, Z. L. Shape Adaptable and Highly Resilient 3D Braided Triboelectric Nanogenerators as E-Textiles for Power and Sensing. *Nat. Commun.* **2020**, *11*, 2868.
- (22) Yu, X.; Pan, J.; Zhang, J.; Sun, H.; He, S.; Qiu, L.; Lou, H.; Sun, X.; Peng, H. A Coaxial Triboelectric Nanogenerator Fiber for Energy Harvesting and Sensing under Deformation. *J. Mater. Chem. A* **2017**, *5*, 6032–6037.
- (23) Lai, Y.-C.; Deng, J.; Zhang, S. L.; Niu, S.; Guo, H.; Wang, Z. L. Single-Thread-Based Wearable and Highly Stretchable Triboelectric Nanogenerators and Their Applications in Cloth-Based Self-Powered Human-Interactive and Biomedical Sensing. *Adv. Funct. Mater.* **2017**, *27*, 1604462.
- (24) Kim, K. N.; Chun, J.; Kim, J. W.; Lee, K. Y.; Park, J.-U.; Kim, S.-W.; Wang, Z. L.; Baik, J. M. Highly Stretchable 2D Fabrics for Wearable Triboelectric Nanogenerator under Harsh Environments. *ACS Nano* **2015**, *9*, 6394–6400.
- (25) Tian, Z.; He, J.; Chen, X.; Wen, T.; Zhai, C.; Zhang, Z.; Cho, J.; Chou, X.; Xue, C. Core-Shell Coaxially Structured Triboelectric Nanogenerator for Energy Harvesting and Motion Sensing. *RSC Adv.* **2018**, *8*, 2950–2957.
- (26) Liu, J.; Cui, N.; Du, T.; Li, G.; Liu, S.; Xu, Q.; Wang, Z.; Gu, L.; Qin, Y. Coaxial Double Helix Structured Fiber-Based Triboelectric Nanogenerator for Effectively Harvesting Mechanical Energy. *Nano-scale Adv.* **2020**, *2*, 4482–4490.
- (27) Cheng, Y.; Lu, X.; Hoe Chan, K.; Wang, R.; Cao, Z.; Sun, J.; Wei Ho, G. A Stretchable Fiber Nanogenerator for Versatile Mechanical Energy Harvesting and Self-Powered Full-Range Personal Healthcare Monitoring. *Nano Energy* **2017**, *41*, 511–518.

- (28) Lin, Z.; He, Q.; Xiao, Y.; Zhu, T.; Yang, J.; Sun, C.; Zhou, Z.; Zhang, H.; Shen, Z.; Yang, J.; Wang, Z. L. Flexible Timbo-Like Triboelectric Nanogenerator as Self-Powered Force and Bend Sensor for Wireless and Distributed Landslide Monitoring. *Adv. Mater. Technol.* **2018**, *3*, 1800144.
- (29) Xiong, J.; Thangavel, G.; Wang, J.; Zhou, X.; Lee, P. S. Self-Healable Sticky Porous Elastomer for Gas-Solid Interacted Power Generation. *Sci. Adv.* **2020**, *6*, No. eabb4246.
- (30) Cheng, B.; Ma, J.; Li, G.; Bai, S.; Xu, Q.; Cui, X.; Cheng, L.; Qin, Y.; Wang, Z. L. Mechanically Asymmetrical Triboelectric Nanogenerator for Self-Powered Monitoring of *In Vivo* Microscale Weak Movement. *Adv. Energy Mater.* **2020**, *10*, 2000827.
- (31) Hinchet, R.; Ghaffarinejad, A.; Lu, Y.; Hasani, J. Y.; Kim, S.-W.; Basset, P. Understanding and Modeling of Triboelectric-Electret Nanogenerator. *Nano Energy* **2018**, *47*, 401–409.
- (32) Gong, S.; Zhang, J.; Wang, C.; Ren, K.; Wang, Z. L. A Monocharged Electret Nanogenerator-Based Self-Powered Device for Pressure and Tactile Sensor Applications. *Adv. Funct. Mater.* **2019**, *29*, 1807618.
- (33) Zhong, J.; Zhong, Q.; Zang, X.; Wu, N.; Li, W.; Chu, Y.; Lin, L. Flexible PET/EVA-Based Piezoelectret Generator for Energy Harvesting in Harsh Environments. *Nano Energy* **2017**, *37*, 268–274.
- (34) Zhang, Y.; Bowen, C. R.; Ghosh, S. K.; Mandal, D.; Khanbareh, H.; Arafa, M.; Wan, C. Ferroelectret Materials and Devices for Energy Harvesting Applications. *Nano Energy* **2019**, *57*, 118–140.
- (35) Mo, X.; Zhou, H.; Li, W.; Xu, Z.; Duan, J.; Huang, L.; Hu, B.; Zhou, J. Piezoelectrets for Wearable Energy Harvesters and Sensors. *Nano Energy* **2019**, *65*, 104033.
- (36) Tsai, J.-W.; Wang, J.-J.; Su, Y.-C. Piezoelectric Rubber Films for Human Physiological Monitoring and Energy Harvesting. *26th IEEE International Conference on Micro Electro Mechanical Systems (Mems)*, 2013; pp 841–844.
- (37) Li, W.; Duan, J.; Zhong, J.; Wu, N.; Lin, S.; Xu, Z.; Chen, S.; Pan, Y.; Huang, L.; Hu, B.; Zhou, J. Flexible THV/COC Piezoelectret Nanogenerator for Wide-Range Pressure Sensing. *ACS Appl. Mater. Interfaces* **2018**, *10*, 29675–29683.
- (38) Mahanty, B.; Ghosh, S. K.; Garain, S.; Mandal, D. An Effective Flexible Wireless Energy Harvester/Sensor Based on Porous Electret Piezoelectric Polymer. *Mater. Chem. Phys.* **2017**, *186*, 327–332.
- (39) Ghosh, S. K.; Biswas, A.; Sen, S.; Das, C.; Henkel, K.; Schmeisser, D.; Mandal, D. Yb³⁺ Assisted Self-Polarized PVDF Based Ferroelectretic Nanogenerator: A Facile Strategy of Highly Efficient Mechanical Energy Harvester Fabrication. *Nano Energy* **2016**, *30*, 621–629.
- (40) Wang, B.; Liu, C.; Xiao, Y.; Zhong, J.; Li, W.; Cheng, Y.; Hu, B.; Huang, L.; Zhou, J. Ultrasensitive Cellular Fluorocarbon Piezoelectret Pressure Sensor for Self-Powered Human Physiological Monitoring. *Nano Energy* **2017**, *32*, 42–49.
- (41) Zhong, J.; Ma, Y.; Song, Y.; Zhong, Q.; Chu, Y.; Karakurt, I.; Bogy, D. B.; Lin, L. A Flexible Piezoelectret Actuator/Sensor Patch for Mechanical Human-Machine Interfaces. *ACS Nano* **2019**, *13*, 7107–7116.
- (42) Fan, F.-R.; Tian, Z.-Q.; Wang, Z. L. Flexible Triboelectric Generator. *Nano Energy* **2012**, *1*, 328–334.
- (43) He, X.; Zi, Y.; Guo, H.; Zheng, H.; Xi, Y.; Wu, C.; Wang, J.; Zhang, W.; Lu, C.; Wang, Z. L. A Highly Stretchable Fiber-Based Triboelectric Nanogenerator for Self-Powered Wearable Electronics. *Adv. Funct. Mater.* **2017**, *27*, 1604378.
- (44) Dong, K.; Deng, J.; Ding, W.; Wang, A. C.; Wang, P.; Cheng, C.; Wang, Y.-C.; Jin, L.; Gu, B.; Sun, B.; Wang, Z. L. Versatile Core-Sheath Yarn for Sustainable Biomechanical Energy Harvesting and Real-Time Human-Interactive Sensing. *Adv. Energy Mater.* **2018**, *8*, 1801114.
- (45) Gong, W.; Hou, C.; Guo, Y.; Zhou, J.; Mu, J.; Li, Y.; Zhang, Q.; Wang, H. A Wearable, Fibroid Self-Powered Active Kinematic Sensor Based on Stretchable Sheath-Core Structural Triboelectric Fibers. *Nano Energy* **2017**, *39*, 673–683.